

# Total gluon shadowing due to fluctuation effects

Misha Kozlov\* and Arif I. Shoshi†

*Fakultät für Physik, Universität Bielefeld, D-33501 Bielefeld, Germany*

Bo-Wen Xiao‡

*Department of Physics, Columbia University, New York, NY, 10027, USA*

We show a new physical phenomenon expected for the ratio  $R_{pA}$  of the unintegrated gluon distribution of a nucleus over the unintegrated gluon distribution of a proton scaled up by the atomic factor  $A^{1/3}$  in the fluctuation-dominated (diffusive scaling) region at high energy. We calculate the dependence of  $R_{pA}$  on the atomic number  $A$ , the rapidity  $Y$  and the transverse gluon momentum  $k_{\perp}$ . We find that  $R_{pA}$  exhibits an increasing gluon shadowing with growing rapidity, approaching  $1/A^{1/3}$  at asymptotic rapidities which means total gluon shadowing, due to the effect of gluon number fluctuations or Pomeron loops. The increase of  $R_{pA}$  with rising gluon momentum decreases as the rapidity grows. In contrast, in the geometric scaling region where the effect of fluctuations is negligible, the ratio  $R_{pA}$  shows only partial gluon shadowing in the fixed-coupling case, basically independent on the rapidity and the gluon momentum.

PACS numbers: 12.38.-t, 12.40.Ee, 24.85.+p

## I. INTRODUCTION

There has been a tremendous progress towards understanding gluon number fluctuation or Pomeron loop effects in the high energy evolution in QCD over the last two years. QCD evolution equations have been established, sometimes called "Pomeron loop equations" [1, 2, 3], which take into account fluctuations and a relation between high density QCD and reaction-diffusion processes in statistical physics has been found which allows us to obtain universal, analytical results for scattering amplitudes in the fluctuation-dominated regime at high energy [2, 4, 5]. The main result, as a consequence of fluctuations, is the emerge of a new scaling behaviour for the dipole-hadron (proton or nucleus) scattering amplitude at high rapidities [5, 6], different from the geometric scaling behaviour which is the hallmark of the "mean field" evolution equations (JIMWLK [7] and BK [8, 9] equations), and which is named *diffusive scaling* by the authors of Ref. [10]. The effect of fluctuations on the scattering amplitude [11, 12, 13, 14, 15, 16, 17, 18, 19, 20, 21, 22, 23], the diffractive scattering processes [10, 24, 25, 26] and gluon production in hadronic scattering processes [27, 28] has been studied so far. In this work we focus on the consequences of fluctuations on the ratio  $R_{pA}$  of the unintegrated gluon distribution of a nucleus over the unintegrated gluon distribution of a proton scaled up by the atomic factor  $A^{1/3}$ .

The "Pomeron loop equations" describing the evolution of the dipole-hadron scattering amplitude with increasing rapidity  $Y = \ln(1/x)$  are stochastic equations. In a frame where most of the rapidity is given to the hadron, the stochastic evolution of the hadron gives rise to different gluon distributions from one event to another [5]. The random variable in the evolution, the logarithm of the saturation momentum  $\rho_s(A, Y) = \ln(Q_s^2(Y)/k_0^2)$ , can therefore vary in an event by event basis. This variation is characterized by the dispersion  $\sigma^2 = \langle \rho_s^2 \rangle - \langle \rho_s \rangle^2$  which rises linearly with rapidity,  $\sigma^2(Y) = D_{dc} \bar{\alpha}_s Y$ , with  $D_{dc}$  the dispersion coefficient and  $\bar{\alpha}_s = \alpha_s N_c / \pi$ . For rapidities  $Y < Y_{DS}$ , the dispersion is small  $\sigma^2 \ll 1$ , meaning that the effect of fluctuations on the scaling form of the unintegrated gluon distribution can be neglected, while for  $Y > Y_{DS}$ , where  $\sigma^2 \gg 1$ , fluctuations become important and do change the scaling form of the unintegrated gluon distribution. We will calculate the gluon distribution of the proton and the nucleus in the geometric scaling region at  $Y < Y_{DS}$  and in the diffusive scaling region at  $Y > Y_{DS}$  which are need in order to study  $R_{pA}$  as a function of the atomic number  $A$ , the rapidity  $Y$  and the transverse gluon momentum  $k_{\perp}$ . All calculations which are presented in this work are valid in the case of a fixed coupling  $\alpha_s$ .

---

\*Electronic address: mkozlov@physik.uni-bielefeld.de

†Electronic address: shoshi@physik.uni-bielefeld.de

‡Electronic address: bowen@phys.columbia.edu

In the overlapping geometric scaling regime of the proton and the nucleus  $R_{pA}$  has been studied by using the JIMWLK or BK equations [29, 30, 31, 32, 33, 34, 35, 36]. It was found [33, 36] that  $R_{pA}$  scales with  $A$  like  $A^{1/3(\gamma_c-1)}$  in the fixed-coupling case, rather than being equal to one ( $\gamma_c = 0.6275$ ) as in the standard pQCD region at very large gluon momenta. This is partial gluon shadowing due to the anomalous behaviour of the unintegrated gluon distribution which stems from the BFKL evolution. Partial gluon shadowing may explain why particle production in heavy ion collisions scales, roughly, like  $N_{part}$  [37]. Furthermore  $R_{pA}$  turns out basically  $k_\perp^2$  and  $Y$  independent in the common geometric scaling regime. The explanation is that the unintegrated gluon distributions of the nucleus and of the proton preserve their shapes with rising rapidity in the geometric scaling regime, yielding thus a constant value for their ratio, as shown for two different rapidities in Fig. 2(a). We will derive the known results in the geometric scaling regime in this work in order to have a direct comparison with the results in the diffusive scaling regime.

We have found that in the overlapping diffusive scaling regime of the proton and the nucleus  $R_{pA}$  basically behaves, for a fixed coupling, as

$$R_{pA} \simeq A^{\frac{1}{3}(\frac{\Delta\rho_s}{2\sigma^2}-1)} \left[ \frac{k_\perp^2}{\langle Q_s(A, Y) \rangle^2} \right]^{\frac{\Delta\rho_s}{\sigma^2}} \quad (1)$$

where  $\Delta\rho_s$  denotes the difference between the average saturation lines of the nucleus and the proton and  $\langle Q_s(A, Y) \rangle$  is the average saturation momentum of the nucleus. This ratio shows two features which are different as compared to the ratio in the geometric scaling regime: (i) For  $k_\perp^2$  close to  $\langle Q_s(A, Y) \rangle^2$ , the gluon shadowing characterized by  $A^{\frac{1}{3}(\frac{\Delta\rho_s}{2\sigma^2}-1)}$  is dominated by fluctuations, through  $\sigma^2(Y)$ , and depends also on the difference  $\Delta\rho_s$ . Gluon shadowing increases as the rapidity increases because of  $\sigma^2 = D_{dc}\bar{\alpha}_s Y$ . At asymptotic rapidity, where  $\sigma^2 \rightarrow \infty$ , one obtains *total gluon shadowing*,  $R_{pA} = 1/A^{1/3}$ , which means that the unintegrated gluon distribution of the nucleus and that of the proton become the same in the diffusive scaling regime. Total gluon shadowing is an effect of fluctuations since the fluctuations make the unintegrated gluon distributions of the nucleus and of the proton flatter and flatter [5] and their ratio closer and closer to 1 (at fixed  $\Delta\rho_s$ ) with rising rapidity as illustrated in Fig.2(b). (Total gluon shadowing is not possible in the geometric scaling regime in the fixed-coupling case since the shapes of the gluon distributions of the nucleus and of the proton remain the same with increasing  $Y$  giving for their ratio a value unequal one, see Fig 2(a)). (ii)  $R_{pA}$  shows an increase with rising  $k_\perp^2$  (always  $R_{pA} < 1$ ) within the diffusive scaling region. Since the exponent  $\Delta\rho_s/\sigma^2$  decreases with rapidity, the slope of  $R_{pA}$  as a function of  $k_\perp^2$  becomes smaller with increasing  $Y$ . The behaviour of  $R_{pA}$  as a function of  $k_\perp$  with increasing rapidity in the diffusive scaling regime is shown in Fig. 3.

The JIMWLK [7] or BK [8, 9] equations, with the geometric scaling being their main consequence, appear to be appropriate for the understanding of the physics explored at RHIC and HERA experiments. However, it may be that this isn't the case anymore at LHC energies where fluctuations may start becoming nonnegligible. Therefore, in addition to the theoretically interesting results for  $R_{pA}$  as a consequence of fluctuations, our result for  $R_{pA}$  may also become relevant in the range of LHC energy. If this is the case, then the increase of the gluon shadowing and the decrease as a function of the gluon momentum of  $R_{pA}$  with rising rapidity as given by Eq. (1) may be viewed as signatures for the onset of fluctuation effects in the LHC data.

This work is organized as follows: In Sec. II we show two different definitions of the unintegrated gluon distributions used in the literature, define  $R_{pA}$  and discuss the initial conditions for the proton and nucleus gluon distributions. In Sec. III we show the results for the gluon distribution of the proton and the nucleus in the geometric and diffusive scaling regime. In Sec. IV we briefly review the known results for the ratio  $R_{pA}$  in the geometric scaling regime, then calculate and discuss the new results for  $R_{pA}$  in the diffusive scaling regime.

## II. GENERALITIES; DEFINITIONS, INITIAL CONDITIONS

In this section we show two different definitions for the unintegrated gluon distribution used in the literature, define the ratio  $R_{pA}$  and describe the initial conditions we use for the unintegrated gluon distribution of the proton and the nucleus.

### A. Definition of unintegrated gluon distributions and $R_{pA}$

Both definitions of the unintegrated gluon distributions of a hadron (proton or nucleus) known in the literature are expressed in terms of the forward scattering amplitude  $N(x_\perp, b_\perp, Y)$  of a QCD dipole of transverse size  $x_\perp$  with rapidity  $Y = \ln 1/x$  scattering off a hadron at impact parameter  $b_\perp$ . Hereafter we consider the scattering process at a fixed impact parameter and omit therefore the  $b_\perp$ -dependence in all the following formulae.

The following definition has been proposed in Ref. [38] for the unintegrated gluon distribution:

$$h_A(k_\perp, Y) = \frac{N_c}{(2\pi)^3 \alpha_s} \int d^2 x_\perp e^{ik_\perp \cdot x_\perp} \nabla_{x_\perp}^2 N(x_\perp, Y), \quad (2)$$

$$= \frac{N_c}{(2\pi)^3 \alpha_s} k_\perp^2 \nabla_{k_\perp}^2 \int \frac{d^2 x_\perp}{x_\perp^2} e^{ik_\perp \cdot x_\perp} N(x_\perp, Y). \quad (3)$$

This formula usually appears in cross sections for gluon production in proton-nucleus collisions [35]. The inversion of Eq. (2) being

$$N(x_\perp, Y) = \frac{(2\pi)^3 \alpha_s}{2N_c} \int \frac{d^2 k_\perp}{(2\pi)^2 k_\perp^2} h_A(k_\perp, Y) (2 - e^{ik_\perp \cdot x_\perp} - e^{-ik_\perp \cdot x_\perp}) \quad (4)$$

does show more explicitly the relation between  $h_A(k_\perp, Y)$  and the dipole-nucleus scattering amplitude: The phase factors in the bracket are due to the four graphs describing the different ways of gluon exchange between the quark and antiquark of the dipole and the hadron.

The other definition of the unintegrated gluon distribution reads

$$\varphi_A(k_\perp, Y) = \frac{N_c}{(2\pi)^3 \alpha_s} \int \frac{d^2 x_\perp}{x_\perp^2} e^{ik_\perp \cdot x_\perp} N(x_\perp, Y) \quad (5)$$

and is derived from the non-Abelian Weizsacker-Williams field of a nucleus [39, 40, 41]. This distribution counts the number of gluons in the wavefunction of the hadron. The two distributions are related to each other by

$$h_A(k_\perp, Y) = k_\perp^2 \nabla_{k_\perp}^2 \varphi_A(k_\perp, Y). \quad (6)$$

The main result of this work, the ratio  $R_{pA}$  in the diffusive scaling regime, turns out to be basically the same for both distributions, as shown in Sec. IV. Some more elaborate discussion on the two different definitions of the unintegrated gluon distribution can be found in Refs. [30, 33].

The quantity which we study in this work is the ratio of the unintegrated gluon distribution of a nucleus over the unintegrated gluon distribution of a proton scaled up by  $A^{1/3}$ ,

$$R_{pA}^h = \frac{h_A(k_\perp, Y)}{A^{1/3} h_p(k_\perp, Y)} \quad \text{and} \quad R_{pA}^\varphi = \frac{\varphi_A(k_\perp, Y)}{A^{1/3} \varphi_p(k_\perp, Y)}, \quad (7)$$

which is a measure of the ratio of the number of particles produces in a proton-nucleus collisions and the corresponding number in proton-proton collisions scaled up by the number of collisions [27, 30, 31, 32, 33, 35].

## B. Initial condition in the case of a nucleus

The evolution of the unintegrated gluon distributions is given by the QCD evolution equations. However, one has to know the initial condition for the unintegrated gluon distribution to start with in the evolution equations. In the case of a nucleus, as an initial condition we use the McLerran-Venugopalan model [44] at fixed  $b_\perp$  and  $Y = 0$ ,

$$N_{MV}(x_\perp, Y = 0) = 1 - \exp\left(-\frac{x_\perp^2 Q_s^2(A)}{4}\right), \quad (8)$$

with the saturation momentum given by [44]

$$Q_s^2(A) = \frac{2\pi^2 \alpha_s}{N_c} \rho T(b) xG\left(x, \frac{1}{x_\perp^2}\right) \quad (9)$$

where  $\rho$  is the nuclear density,  $T(b) = 2\sqrt{R_A^2 - b^2}$  is the profile function and  $xG(x, 1/x_\perp^2)$  is the gluon distribution in the nucleon which at  $Y = 0$  can be written as  $xG(x = 1, 1/x_\perp^2) \propto \alpha_s \ln(1/x_\perp^2 \Lambda_{QCD}^2)$ . Since we are interested throughout this work in the region where  $1/x_\perp$  is not much larger than the saturation scale  $Q_s^2(A)$ , we neglect the  $x_\perp$

by replacing it by  $1/Q_s^2(A)$  in  $xG(x, 1/x_\perp^2)$ . Noting also that  $\rho T(b) \propto Q_0^2 A^{1/3}$  at fixed impact parameter, one gets for the  $\alpha_s$  and  $A$  dependence

$$Q_s^2(A) \propto Q_0^2 \alpha_s^2 A^{\frac{1}{3}} \ln(\alpha_s^2 A^{1/3}) \quad (10)$$

which has also been used in Refs. [27, 36]. We shall always assume that  $\alpha_s^2 A^{\frac{1}{3}} \gg 1$  in order to have non-trivial nuclear effects.

Using the Mellin transform of the scattering amplitude,

$$N_{MV}(\gamma) = \int_0^\infty du u^{-\gamma-1} [1 - \exp(-u)] = -\Gamma(-\gamma) \quad \text{with } 0 < \gamma < 1 \quad (11)$$

where  $u = \frac{x_\perp^2 Q_s^2(A)}{4}$ , one can write Eq. (8) also in the form

$$N_{MV}(x_\perp, Y=0) = \int \frac{d\gamma}{2\pi i} N_{MV}(\gamma) \exp \left[ \gamma \ln \left( \frac{x_\perp^2 Q_s^2(A)}{4} \right) \right], \quad (12)$$

which together with Eq. (2) and Eq. (5) allows us to get the unintegrated gluon distribution of a nucleus at  $Y=0$ ,

$$h_A(k_\perp, Y=0) = \frac{N_c}{2\pi^2 \alpha_s} \left( \frac{k_\perp^2}{Q_s^2(A)} \right) \exp \left( -\frac{k_\perp^2}{Q_s^2(A)} \right), \quad (13)$$

$$\varphi_A(k_\perp, Y=0) = \frac{N_c}{8\pi^2 \alpha_s} \Gamma \left( 0, \frac{k_\perp^2}{Q_s^2(A)} \right), \quad (14)$$

where  $\Gamma \left( 0, \frac{k_\perp^2}{Q_s^2(A)} \right) \simeq \ln \left( \frac{k_\perp^2}{Q_s^2(A)} \right) - \gamma_E + \frac{k_\perp^2}{Q_s^2(A)} + \dots$  is the incomplete Gamma function.

Let us also construct the expressions for unintegrated gluon distributions which take into account BFKL evolution since they turn out to be useful in the next sections. This is easily done by starting with the BFKL evolved scattering amplitude in terms of the Mellin transform

$$N_{MV}(x_\perp, Y) = \int_{c-i\infty}^{c+i\infty} \frac{d\gamma}{2\pi i} N_{MV}(\gamma) \exp \left[ \bar{\alpha}_s Y \chi(\gamma) + \gamma \ln \left( \frac{x_\perp^2 Q_s^2(A)}{4} \right) \right] \quad (15)$$

where  $0 < c < 1$ ,  $\bar{\alpha}_s = \frac{\alpha_s N_c}{\pi}$  and  $\chi(\gamma) = 2\psi(1) - \psi(\gamma) - \psi(1-\gamma)$  with  $\psi(\gamma)$  a polygamma function. With Eq.(15) inserted into Eq.(2) and Eq.(5) and the relation

$$\int \frac{d^2 x_\perp}{x_\perp^2} e^{ik_\perp \cdot x_\perp} \left( \frac{x_\perp^2 Q_s^2(A)}{4} \right)^\gamma = \pi \frac{\Gamma(\gamma)}{\Gamma(-\gamma+1)} \left( \frac{k_\perp^2}{Q_s^2(A)} \right)^{-\gamma} \quad (16)$$

one obtains the Mellin representation of the unintegrated gluon distributions which contain rapidity evolution:

$$h_A(k_\perp, Y) = \frac{N_c}{2\pi^2 \alpha_s} \int_{c-i\infty}^{c+i\infty} \frac{d\gamma}{2\pi i} \Gamma(\gamma+1) \exp \left[ \bar{\alpha}_s Y \chi(\gamma) - \gamma \ln \left( \frac{k_\perp^2}{Q_s^2(A)} \right) \right]; \quad (17)$$

$$\varphi_A(k_\perp, Y) = \frac{N_c}{8\pi^2 \alpha_s} \int_{c-i\infty}^{c+i\infty} \frac{d\gamma}{2\pi i} \frac{\Gamma(\gamma)}{\gamma} \exp \left[ \bar{\alpha}_s Y \chi(\gamma) - \gamma \ln \left( \frac{k_\perp^2}{Q_s^2(A)} \right) \right]. \quad (18)$$

In the limit of  $Y=0$  Eq. (15), Eq. (17) and Eq. (18) reduce, of course, to Eq.(12), Eq.(13) and Eq.(14) respectively.

### C. Initial condition in the case of a proton

We use two different ways to describe the initial gluon distribution of the proton: (i) In the main body of this work we view the proton as a single color dipole (see also Ref. [36]) and (ii) in Appendix A we view the proton as a composite object and use the McLerran-Venugopalan model to describe its initial conditions (see also Ref. [33]). We will show that both point of views exhibit equally well the effect of fluctuations on  $R_{pA}$  which is the main focus of this work.

The scattering amplitude for a dipole of size  $x_\perp$  scattering off a dipole of size  $x'_\perp$  at relative rapidity  $Y$  reads [43]

$$N(x'_\perp, x_\perp, Y) = \pi \alpha_s^2 x'_\perp{}^2 \int_{c-i\infty}^{c+i\infty} \frac{d\gamma}{2\pi i} \frac{1}{\gamma^2(1-\gamma)^2} \exp \left[ \bar{\alpha}_s \chi(\lambda) Y - \gamma \ln \frac{x'_\perp{}^2}{x_\perp^2} \right] \quad (19)$$

where  $0 < c < 1$ . When  $Y = 0$  the above expression reduces to the dipole-dipole scattering amplitude at the two gluon exchange level

$$N(x'_\perp, x_\perp, Y = 0) = 2\pi \alpha_s^2 r_{<}^2 \left( 1 + \ln \frac{r_{>}}{r_{<}} \right) \quad (20)$$

with  $r_{<}$  being the smaller of  $x_\perp, x'_\perp$  and  $r_{>}$  the larger of  $x_\perp, x'_\perp$ .

Following the same steps as in the case of a nucleus, one obtains for the unintegrated gluon distributions of a proton which take into account BFKL evolution

$$h_p(k_\perp, Y) = \frac{N_c}{2\pi^2 \alpha_s} \pi \alpha_s^2 x_\perp'^2 \int_{c-i\infty}^{c+i\infty} \frac{d\gamma}{2\pi i} \frac{4^\gamma}{(1-\gamma)^2} \frac{\Gamma(\gamma)}{\Gamma(1-\gamma)} \exp [\bar{\alpha}_s Y \chi(\gamma) - \gamma \ln(k_\perp^2 x_\perp'^2)]; \quad (21)$$

$$\varphi_p(k_\perp, Y) = \frac{N_c}{8\pi^2 \alpha_s} \pi \alpha_s^2 x_\perp'^2 \int_{c-i\infty}^{c+i\infty} \frac{d\gamma}{2\pi i} \frac{4^\gamma}{\gamma^2(1-\gamma)^2} \frac{\Gamma(\gamma)}{\Gamma(1-\gamma)} \exp [\bar{\alpha}_s Y \chi(\gamma) - \gamma \ln(k_\perp^2 x_\perp'^2)] . \quad (22)$$

The Eqs. (17), (18) and Eqs. (21), (22) have the form of the formulae one has started with in Ref. [43] and Ref. [5, 6] to study the geometric scaling region and the diffusive scaling region. These equations tell us what the effect of the different initial conditions is according to Ref. [5, 6, 43]: Different initial conditions for the proton as compared with the ones for the nucleus do lead to different saturation momenta,  $Q_s(p, Y)$  unequal  $Q_s(A, Y)$ . The saturation momentum does slightly depend also on the definition for the unintegrated gluon distribution,  $h_{p,A}(k_\perp, Y)$  and  $\varphi_{p,A}(k_\perp, Y)$ . In the next section we do show the exact expressions of the saturation momentum of the proton and the nucleus.

### III. UNINTEGRATED GLUON DISTRIBUTION OF A HADRON

In this section we focus on the unintegrated gluon distribution of a highly evolved hadron (nucleus or proton) in the geometric and diffusive scaling region. To explain the relevant physics in these two regions let us look at the phase diagram of the hadron in the high-energy limit shown in the  $Y - \rho$  plane in Fig. 1. Here  $Y = \ln(1/x)$  is the rapidity of the hadron and  $\rho = \ln(k_\perp^2/k_0^2)$  is the logarithm of the transverse momentum of gluons inside the hadron ( $k_0^2$  is a fixed reference scale). The straight line denoted by  $\langle \rho_s(A, Y) \rangle$  represents the average saturation line,  $\langle \rho_s(A, Y) \rangle = \langle \ln(Q_s(A, Y)/k_0^2) \rangle$ , with the saturation momentum  $Q_s(A, Y)$  depending on  $Y$  and the atomic number  $A$ . To the left of the saturation line,  $\rho < \langle \rho_s(A, Y) \rangle$ , the gluon density is of order  $1/\alpha_s$ , or, the dipole-hadron scattering amplitude is at the unitarity limit  $\langle N \rangle \approx 1$ . In this region, called "saturation region", the nonlinear QCD evolution becomes important. For  $\rho \gg \langle \rho_s(A, Y) \rangle$ , the gluon density is low and the standard 'double-logarithmic approximation' is applicable. In the low density regime neither saturation nor fluctuation effects are important and the unintegrated gluon distribution behaves as  $1/k_\perp^2$  at very large  $k_\perp$  (the amplitude shows color transparency,  $\langle N(r_\perp) \rangle \propto r_\perp^2$ ). The most interesting region for us in this work is the transition region between the saturation and the low density regime where  $\rho$  is not much larger than  $\langle \rho_s(A, Y) \rangle$  (see Fig. 1). There are two different regimes within the transition region which are separated by the rapidity scale  $Y_{DS}$ , the *geometric scaling regime* [4, 42, 43] and the *diffusive scaling regime* [5, 6], in which the dynamics of the QCD evolution is different.

The QCD evolution of the dipole-hadron scattering amplitude with increasing rapidity  $Y = \ln(1/x)$  is stochastic [5, 6] meaning that the scattering amplitude can fluctuate from event to event. Equivalently, in a frame where most of the rapidity is given to the hadron, the stochastic evolution of the hadron gives rise to different gluon distributions from one event to another [5]. Therefore the random variable,  $\rho_s(A, Y) = \ln(Q_s^2(A, Y)/k_0^2)$ , can vary from one event to another. Its variation is characterized by the dispersion  $\sigma^2 = \langle \rho_s^2 \rangle - \langle \rho_s \rangle^2$  which rises linearly with rapidity,  $\sigma^2(Y) = D_{dc} \bar{\alpha}_s Y$ , with  $D_{dc}$  the dispersion coefficient. For rapidities  $Y < Y_{DS}$ , the dispersion is small  $\sigma^2 \ll 1$ , meaning that the effect of fluctuations on the scaling form of the unintegrated gluon distribution can be neglected, while for  $Y > Y_{DS}$ , where  $\sigma^2 \gg 1$ , fluctuations become important and do change the scaling form of the unintegrated gluon distribution as we show below (see also Ref. [10, 27] for more discussions on the phase diagram).

#### A. Geometric scaling regime

In the geometric scaling regime at  $Y \ll Y_F$  ( $Y_F$  will be fixed below, see also Fig. 1) the QCD evolution is described by the Kovchegov equation [9], or, equivalently, by the BFKL equation in the presence of a saturation boundary [4, 43]. Starting with Eq. (17) and following the calculations in Refs. [4, 43] one finds for the unintegrated gluon distribution of a nucleus in the case of a fixed coupling

$$h_A(k_\perp, Y) = h_A^{\max} \gamma_c \left( \frac{k_\perp^2}{Q_s^2(A, Y)} \right)^{-\gamma_c} \left[ \ln \left( \frac{k_\perp^2}{Q_s^2(A, Y)} \right) + \frac{1}{\gamma_c} \right] \quad (23)$$

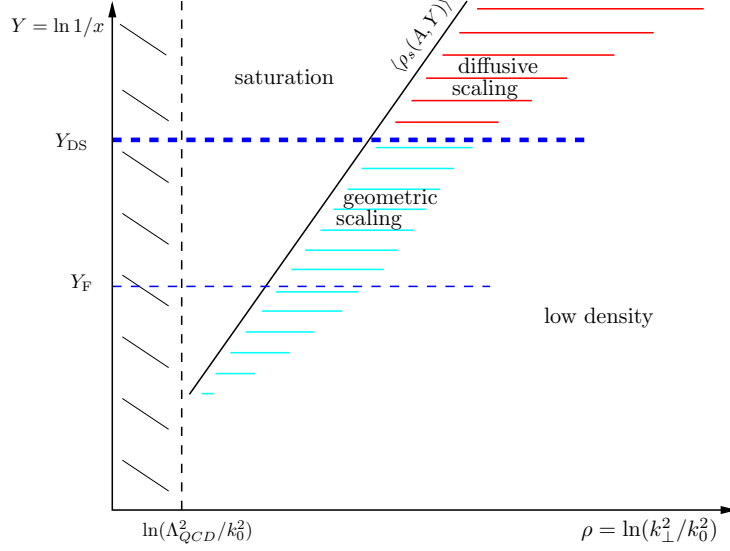


FIG. 1: The phase diagram of the unintegrated gluon distribution of a proton (or nucleus) in the kinematical plane  $Y - \ln(k_\perp^2/k_0^2)$ . The high density region (saturation region) at small gluon momenta is on the left hand side of the saturation line  $\langle \rho_s(A, Y) \rangle$ , the low density region at very high gluon momenta is on the right hand side of shadowed area. The intermediate region separated by  $Y_{DS}$  divides the geometric scaling regime from the diffusive scaling regime.

which is valid in the geometric scaling regime

$$Q_s^2(A) \leq k_\perp^2 \leq Q_s^2(A) \exp \left[ \sqrt{4\chi''(\gamma_c) \bar{\alpha}_s Y} \right]. \quad (24)$$

and scales as a function of the dimensionless variable  $k_\perp^2/Q_s^2(A, Y)$ . The observation of a similar scaling behaviour at the HERA data for DIS at  $x \leq 0.01$  and any momentum [46] supports the theoretical findings. In the above equation  $Q_s^2(A, Y)$  denotes the saturation momentum of the nucleus

$$Q_s^2(A, Y) = c_A^h Q_s^2(A) \frac{\exp[\frac{\chi(\gamma_c)}{\gamma_c} \bar{\alpha}_s Y]}{[2\bar{\alpha}_s Y \chi''(\gamma_c)]^{\frac{3}{2\gamma_c}}}, \quad (25)$$

where  $c_A$  is a constant and the value of the anomalous dimension,  $\gamma_c = 0.6275$ , which comes from the BFKL dynamics in the presence of saturation, is fixed by  $\chi'(\gamma_c) = \frac{\chi(\gamma_c)}{\gamma_c}$ . In Eq. (23)  $h_A^{\max} = \mathcal{O}(1/\alpha_s)$  is the maximum of  $h_A(k_\perp, Y)$  which happens when  $k_\perp^2 = Q_s^2(A, Y)$ .

The unintegrated gluon distribution  $\varphi_A(k_\perp, Y)$ , defined in Eq. (5), has in the geometric scaling regime exactly the same form as  $h_A(k_\perp, Y)$  given in Eq. (23). The only difference, steaming from the different initial conditions at  $Y = 0$ , see eq. (17) and Eq. (18), is a slightly different constant  $c_A^\varphi$  in the saturation momentum.

To get the parametrical estimates for the rapidities  $Y_F$  and  $Y_{DS}$ , it is convenient to express the above results in the geometric scaling regime in terms of the  $\rho = \ln k_\perp^2/k_0^2$  variable,

$$h_A(k_\perp, Y) = h_A^{\max} \gamma_c e^{-\gamma_c(\rho - \rho_s(A, Y))} \left( \rho - \rho_s(A, Y) + \frac{1}{\gamma_c} \right) \quad (26)$$

with the region of validity

$$0 \leq \rho - \rho_s(A, Y) \leq \sqrt{4\chi''(\gamma_c) \bar{\alpha}_s Y} \quad (27)$$

and

$$\rho_s(A, Y) = \ln \frac{c_A^h Q_s^2(A)}{k_0^2} + \frac{\chi(\gamma_c)}{\gamma_c} \bar{\alpha}_s Y - \frac{3}{2\gamma_c} \ln [2\bar{\alpha}_s Y \chi''(\gamma_c)]. \quad (28)$$

Gluon number fluctuations (Pomeron loops) [5, 6] do change the results (26) and (28) which emerge from the Kovchegov equation as the rapidity increases. These results remain valid so long as the gluon occupancy in the nucleus,  $n(k_\perp, Y) \propto h_A(k_\perp, Y)/\alpha_s$ , is much larger than one in the geometric scaling regime. When  $n(k_\perp, Y) \approx O(1)$  (or the scattering amplitude  $N(r, Y) \approx \alpha_s^2 n(k \sim 1/r, Y)$ ) the discreteness of the gluons has to be taken into account, allowing the occupancy to go below one only by becoming zero [5, 6]. The gluon occupancy becomes of order one at the largest  $k_\perp$  within the geometric scaling regime, or  $h_A(k_\perp, Y) \approx \alpha_s$ , when  $\rho - \rho_s \approx \frac{1}{\gamma_c} \ln(1/\alpha_s^2)$ . According to Eq.(27), this happens at the rapidity

$$Y_F \propto \frac{1}{\alpha_s} \ln^2(1/\alpha_s^2) . \quad (29)$$

For  $Y_F \leq Y$  fluctuations do change somewhat  $\rho_s(A, Y)$  given in Eq. (28) to [5, 6]

$$\langle \rho_s(A, Y) \rangle = \ln \frac{c_A^h Q_s^2(A)}{k_0^2} + \left( \frac{\chi(\gamma_c)}{\gamma_c} - \frac{\pi^2 \gamma_c \chi''(\gamma_c)}{2 \ln^2(1/\alpha_s^2)} \right) \bar{\alpha}_s Y . \quad (30)$$

Fluctuations, however, do not change the shape of the unintegrated gluon distribution in Eq. (26) in the region  $Y_F \leq Y \ll Y_{DS}$  because of the following reason: Starting with a unique initial gluon distribution at  $Y = 0$ , the stochastic evolution generates an ensemble of them at rapidity  $Y$ , where each of the individual gluon distributions has the shape given by (26), but the individual gluon distributions may differ from each other by translation ( $\rho_s(A, Y)$  is random). Based on the relation between QCD evolution and reaction-diffusion models in statistical physics [5], the fluctuations are taken into account by averaging over all individual distributions,

$$\langle h_A(\rho - \rho_s(A, Y)) \rangle = \int d\rho_s h_A(\rho - \rho_s(A, Y)) P(\rho_s - \langle \rho_s \rangle) , \quad (31)$$

where the probability distribution of  $\rho_s(A, Y)$  is argued to have a Gaussian form [45],

$$P(\rho_s) \simeq \frac{1}{\sqrt{2\pi\sigma^2}} \exp \left[ -\frac{(\rho_s - \langle \rho_s \rangle)^2}{2\sigma^2} \right] \quad \text{for } \rho - \rho_s(A, Y) \ll \gamma_c^2 \sigma^2 , \quad (32)$$

with the variance

$$\sigma^2 = \langle \rho_s(A, Y)^2 \rangle - \langle \rho_s(A, Y) \rangle^2 = D_{dc} \bar{\alpha}_s Y \quad (33)$$

and the diffusion coefficient at asymptotic energies given by [5, 6]

$$D_{dc} = \frac{\pi^4 \gamma_c \chi''(\gamma_c)}{3 \log^3(1/\alpha_s^2)} . \quad (34)$$

Now, if the variance is small,  $\sigma^2 \ll 1$ , which is the case as long as the rapidity is much smaller than

$$Y_{DS} \simeq \frac{1}{D_{dc} \bar{\alpha}_s} , \quad (35)$$

then the Gaussian distribution in Eq.(32) is strongly peaked and therefore the averaged gluon distribution nearly preserves the form of an individual distribution,

$$\langle h_A(\rho - \rho_s(A, Y)) \rangle \approx h_A(\rho - \langle \rho_s(A, Y) \rangle) \quad (36)$$

and shows geometric scaling, at least in the window  $0 \leq \rho - \rho_s(A, Y) \leq \ln(1/\alpha_s^2)/\gamma_c$ . So, at  $Y \leq Y_F$  the unintegrated gluon distribution in the geometric scaling regime (see Fig. 1) is given by (26) with the saturation momentum given by (28) while at  $Y_F \leq Y \leq Y_{DS}$  the unintegrated gluon distribution remains approximately the same while the saturation momentum changes to the one given in Eq. (30).

The only change in the case of a proton as compared to that of the nucleus in the geometric scaling regime is the saturation momentum,  $\langle \rho_s(A, Y) \rangle \rightarrow \langle \rho_s(p, Y) \rangle$ , which is done by replacing  $c_A^{h,\varphi} Q_s^2(A)$  in the expressions for  $\langle \rho_s(A, Y) \rangle$  by  $c_p^{h,\varphi} Q_s^2(p)$ , where  $c_p^{h,\varphi}$  is a constant and  $Q_s^2(p) x_\perp'^2 = [\alpha_s \sqrt{\ln(1/\alpha_s)}]^{2/\gamma_c}$ . The saturation momenta of the proton and the nucleus are different due to different initial conditions which we have explained in Sect. II B and Sect. II C. The difference between them is

$$\begin{aligned} \Delta \rho_s &\equiv \langle \rho_s(A, Y) \rangle - \langle \rho_s(p, Y) \rangle = \ln \frac{\langle Q_s(A, Y) \rangle^2}{\langle Q_s(p, Y) \rangle^2} \\ &= \ln \frac{c c_A^{h,\varphi} Q_0^2 x_\perp'^2 \alpha_s^2 A^{1/3} \ln(\alpha_s^2 A^{1/3})}{c_p^{h,\varphi} [\alpha_s \sqrt{\ln(1/\alpha_s)}]^{2/\gamma_c}} \end{aligned} \quad (37)$$

with  $c$  a constant. A different  $\Delta\rho_s$  is obtained when the proton is viewed as a composite object, instead of a single dipole, and is described by the McLerran-Vnugopalan model, as done in Appendix A.

## B. Diffusive scaling regime

The diffusive scaling regime sets in when the variance is large,  $\sigma^2 \gg 1$ , which happens at  $Y \gg Y_{DS}$ . In the diffusive scaling regime the fluctuations are very important and the unintegrated gluon distribution changes therefore a lot from one event to another, leading to an average unintegrated gluon distribution  $\langle h_A(\rho - \rho_s(A, Y)) \rangle$  in Eq.(31) which is quite different as compared to the event-by-event gluon distribution  $h_A(\rho - \rho_s(A, Y))$  as we show below.

We use for the event-by-event unintegrated gluon distributions

$$h_A(\rho - \rho_s(A, Y)) = \begin{cases} h_A^{max} \exp[-(\rho_s(A, Y) - \rho)] & \text{for } \rho < \rho_s(A, Y), \\ h_A^{max} \exp[-\gamma_c(\rho - \rho_s(A, Y))] & \text{for } \rho > \rho_s(A, Y) \end{cases} ; \quad (38)$$

$$\varphi_A(\rho - \rho_s(A, Y)) = \begin{cases} \varphi_A^{max} \left[ \frac{1}{2} (\rho_s(A, Y) - \rho) + 1 \right] & \text{for } \rho < \rho_s(A, Y), \\ \varphi_A^{max} \exp[-\gamma_c(\rho - \rho_s(A, Y))] & \text{for } \rho > \rho_s(A, Y) \end{cases} , \quad (39)$$

In the above equations we have used for  $\rho > \rho_s(A, Y)$  the leading contributions valid in the geometric scaling regime (see Sect. III A) while for  $\rho < \rho_s(A, Y)$  (saturation regime) the expressions which come from solving the Kovchegov equation (see Appendix B and [9])<sup>1</sup>. There is a difference between the  $h_A$  and  $\varphi_A$  distributions in the saturation region coming from their different definitions in (2) and (5). (We have used for simplicity the geometric scaling result also in the low density regime, see Fig. 1, where both distributions behave the same way, like  $1/k_\perp^2$ , since the main result in the diffusive scaling regime is insensitive to the low density region.)

It is now easy to show that the average unintegrated gluon distributions are roughly described by Gaussians,

$$\langle h_A(\rho - \rho_s(A, Y)) \rangle \simeq \frac{h_A^{max}}{\sqrt{2\pi\sigma^2}} \left( \frac{1 + \gamma_c}{\gamma_c} \right) \exp \left[ -\frac{(\rho - \langle \rho_s(A, Y) \rangle)^2}{2\sigma^2} \right] , \quad (40)$$

$$\langle \varphi_A(\rho - \rho_s(A, Y)) \rangle \simeq \frac{\varphi_A^{max} \sigma^3}{2\sqrt{2\pi} [\rho - \langle \rho_s(A, Y) \rangle]^2} \exp \left[ -\frac{[\rho - \langle \rho_s(A, Y) \rangle]^2}{2\sigma^2} \right] , \quad (41)$$

and are valid in the diffusive scaling regime,

$$\sigma \ll \rho - \langle \rho_s(A, Y) \rangle \ll \gamma_c \sigma^2 . \quad (42)$$

Note that in the diffusive scaling regime the unintegrated gluon distribution scales as a function of the dimensionless variable  $(\rho - \langle \rho_s \rangle)/\sigma(Y)$  which is different as compared to the geometric scaling  $(\rho - \langle \rho_s \rangle)$ . The diffusive scaling extends up to very large values of gluon momenta  $k_\perp^2$  since the window  $\rho - \langle \rho_s \rangle \ll \sigma^2$  increases with rapidity, see Eq.(33). The same result as the one in Eq. (40) was obtained in Ref. [27], although in a different way, and was shown to give the cross section for gluon production in the diffusive scaling regime.

The geometric (diffusive) scaling window of a proton as compared to the geometric (diffusive) scaling window of a nucleus at high rapidity is shifted to lower momenta due to the smaller saturation momentum of the proton (see (37)). The proton and the nucleus have a common geometric scaling region for rapidities  $Y < Y_{DS}$ . The common diffusive scaling for the proton and the nucleus at  $Y \geq Y_{DS}^{pA}$  sets in when the diffusive scaling window of the proton overlaps with the one of the nucleus,

$$\sigma^2 = D_{dc} \bar{\alpha}_s Y \gg \sigma + \Delta\rho_s \quad (43)$$

which determines

$$Y_{DS}^{pA} \propto \begin{cases} \frac{1}{D_{dc} \bar{\alpha}_s} (\Delta\rho_s)^2 & \text{for } \sigma > \Delta\rho_s \\ \frac{1}{D_{dc} \bar{\alpha}_s} \Delta\rho_s & \text{for } \sigma < \Delta\rho_s . \end{cases} \quad (44)$$

---

<sup>1</sup> The McLerran-Venugopalan model also gives the same expressions as a function of rapidity for  $\rho < \rho_s(A, Y)$ .



#### IV. THE RATIO $R_{pA}$ IN THE GEOMETRIC AND DIFFUSIVE SCALING REGIME

In the geometric scaling regime the unintegrated gluon distributions  $h_A(\rho - \langle \rho_s \rangle)$  and  $\varphi_A(\rho - \langle \rho_s \rangle)$  show the same behaviour (see Sect. III A). From Eqs. (26) and (37) one finds for the ratio  $R_{pA}^{h,\varphi}$  defined in Eq. (7)

$$\begin{aligned} R_{pA}^{h,\varphi}(k_\perp, Y, A) &\simeq \frac{1}{A^{\frac{1}{3}}} \left[ \frac{\langle Q_s(A, Y) \rangle^2}{\langle Q_s(p, Y) \rangle^2} \right]^{\gamma_c} \frac{\ln \left( \frac{k_\perp^2}{\langle Q_s(A, Y) \rangle^2} \right) + \frac{1}{\gamma_c}}{\ln \left( \frac{k_\perp^2}{\langle Q_s(p, Y) \rangle^2} \right) + \frac{1}{\gamma_c}} \\ &\simeq \frac{1}{A^{\frac{1}{3}(1-\gamma_c)}} \frac{[\alpha_s^2 \ln(\alpha_s^2 A^{1/3})]^{\gamma_c}}{\alpha_s^2 \ln(1/\alpha_s)} \left( \frac{c_A^{h,\varphi} c x_\perp'^2 Q_0^2}{c_p^{h,\varphi}} \right)^{\gamma_c} \frac{\ln \left( \frac{k_\perp^2}{\langle Q_s(A, Y) \rangle^2} \right) + \frac{1}{\gamma_c}}{\ln \left( \frac{k_\perp^2}{\langle Q_s(p, Y) \rangle^2} \right) + \Delta \rho_s + \frac{1}{\gamma_c}} \end{aligned} \quad (45)$$

where we have used  $h_A^{max} = h_p^{max}$  and  $\varphi_A^{max} = \varphi_p^{max}$  and the average saturation momentum  $\langle Q_s \rangle^2$  defined via  $\langle \rho_s \rangle \equiv \ln \langle Q_s \rangle^2 / k_0^2$ . For gluon momenta not too far from  $\langle Q_s(A, Y) \rangle$  the ratio  $R_{pA}^{h,\varphi}$  scales with  $A$  like  $A^{1/3(\gamma_c-1)}$ , rather than being equal to one. This is partial gluon shadowing due to the anomalous behaviour of the unintegrated gluon distribution given in Eq. (17) which stems from the BFKL evolution. This result, already derived in Refs. [33, 36], may explain why particle production in heavy ion collisions scales, roughly, like  $N_{part}$  [37]. Moreover  $R_{pA}^{h,\varphi}$  reduces to a  $k_\perp^2$  and  $Y$  independent expression for  $k_\perp^2$  much larger than  $\langle Q_s(A, Y) \rangle^2$ , or  $\ln(k_\perp^2 / \langle Q_s(A, Y) \rangle^2) \gg \Delta \rho_s$ . This comes from the fact that the unintegrated gluon distribution of the nucleus and of the proton preserves the shape with rising rapidity, yielding therefore a constant value for their ratio. This behaviour is shown in Fig. 2(a).

In the diffusive scaling regime the ratio  $R_{pA}$  for the unintegrated gluon distribution in Eq. (40) equals

$$\begin{aligned} R_{pA}^h(k_\perp, Y, A) &= \frac{1}{A^{\frac{1}{3}}} \left[ \frac{\langle Q_s(A, Y) \rangle^2}{\langle Q_s(p, Y) \rangle^2} \right]^{\frac{\Delta \rho_s}{2\sigma^2}} \left[ \frac{k_\perp^2}{\langle Q_s(A, Y) \rangle^2} \right]^{\frac{\Delta \rho_s}{\sigma^2}} \\ &= \frac{1}{A^{\frac{1}{3}(1-\frac{\Delta \rho_s}{2\sigma^2})}} \left[ \frac{\alpha_s^2 \ln(\alpha_s^2 A^{1/3})}{(\alpha_s^2 \ln(1/\alpha_s))^{1/\gamma_c}} \right]^{\frac{\Delta \rho_s}{2\sigma^2}} \left[ \frac{c_A^h c x_\perp'^2 Q_0^2}{c_p^h} \right]^{\frac{\Delta \rho_s}{2\sigma^2}} \left[ \frac{k_\perp^2}{\langle Q_s(A, Y) \rangle^2} \right]^{\frac{\Delta \rho_s}{\sigma^2}} \end{aligned} \quad (46)$$

while for the "Weizsacker-Williams" unintegrated gluon distribution in Eq. (41) it is

$$\begin{aligned} R_{pA}^\varphi &= \frac{1}{A^{\frac{1}{3}}} \left[ \frac{\langle Q_s(A, Y) \rangle^2}{\langle Q_s(p, Y) \rangle^2} \right]^{\frac{\Delta \rho_s}{2\sigma^2}} \left[ \frac{k_\perp^2}{\langle Q_s(A, Y) \rangle^2} \right]^{\frac{\Delta \rho_s}{\sigma^2}} \frac{\left[ \ln \left( \frac{k_\perp^2}{\langle Q_s(A, Y) \rangle^2} \right) + \Delta \rho_s \right]^2}{\left[ \ln \left( \frac{k_\perp^2}{\langle Q_s(p, Y) \rangle^2} \right) \right]^2} \\ &= \frac{1}{A^{\frac{1}{3}(1-\frac{\Delta \rho_s}{2\sigma^2})}} \left[ \frac{\alpha_s^2 \ln(\alpha_s^2 A^{1/3})}{(\alpha_s^2 \ln(1/\alpha_s))^{1/\gamma_c}} \right]^{\frac{\Delta \rho_s}{2\sigma^2}} \left[ \frac{c_A^\varphi c x_\perp'^2 Q_0^2}{c_p^\varphi} \right]^{\frac{\Delta \rho_s}{2\sigma^2}} \left[ \frac{k_\perp^2}{\langle Q_s(A, Y) \rangle^2} \right]^{\frac{\Delta \rho_s}{\sigma^2}} \frac{\left[ \ln \left( \frac{k_\perp^2}{\langle Q_s(A, Y) \rangle^2} \right) + \Delta \rho_s \right]^2}{\left[ \ln \left( \frac{k_\perp^2}{\langle Q_s(p, Y) \rangle^2} \right) \right]^2}. \end{aligned} \quad (47)$$

In the diffusive scaling regime  $R_{pA}^{h,\varphi}$  becomes independent of the definition of the gluon distribution and shows the universal behaviour  $A^{1/3(\frac{\Delta \rho_s}{2\sigma^2}-1)} [k_\perp^2 / \langle Q_s(A, Y) \rangle^2]^{\frac{\Delta \rho_s}{\sigma^2}}$  when  $\ln(k_\perp^2 / \langle Q_s(A, Y) \rangle^2) \gg \Delta \rho_s$ . The above ratios in the diffusive scaling regime show two different features as compared to the ratio in the geometric scaling regime: (i) For  $k_\perp^2$  close to  $\langle Q_s(A, Y) \rangle^2$ , the gluon shadowing characterized by  $A^{1/3(\frac{\Delta \rho_s}{2\sigma^2}-1)}$  is dominated by fluctuations, through  $\sigma^2(Y)$ , and depends also on the difference  $\Delta \rho_s$ . The gluon shadowing increases as the rapidity increases because of  $\sigma^2 = D_{dc} \bar{\alpha}_s Y$ . At asymptotic rapidity, where  $\sigma^2 \rightarrow \infty$ , one obtains *total gluon shadowing*,  $R_{pA}^{h,\varphi} = 1/A^{1/3}$ , which means that the unintegrated gluon distribution of the nucleus and that of the proton become the same in the diffusive scaling regime. The total gluon shadowing is an effect of fluctuations at fixed coupling since the fluctuations make the unintegrated gluon distributions of the nucleus and of the proton flatter and flatter and their ratio closer and closer to 1 (at fixed  $\Delta \rho_s$ ) with rising rapidity, as shown in Fig. 2(b). (ii)  $R_{pA}^{h,\varphi}$  shows an increase with rising  $k_\perp^2$  within the diffusive scaling region. Since the exponent  $\Delta \rho_s / \sigma^2$  decreases with rapidity, the slope of  $R_{pA}^{h,\varphi}$  as a function of  $k_\perp^2$  becomes smaller with increasing  $Y$ . Both features of  $R_{pA}$  in the diffusive scaling regime, the increasing gluon shadowing and the decreasing  $k_\perp$  dependence with rising rapidity, are shown in Fig. 3. Note also that in the common diffusive scaling regime, see (42) and (43), the ratio  $R_{pA}$  is always smaller than one. (This can be seen especially from Eq.(A5) where  $\Delta \rho_s = \ln A^{1/3}$  was used.)

Total gluon shadowing is not possible in the geometric scaling regime in the fixed-coupling case since the shapes of the gluon distributions of the nucleus and of the proton remain the same with increasing  $Y$  giving for their ratio a

value unequal one (see Fig 2(a)). In the case of a running coupling, the gluon shadowing increases with rising rapidity in the geometric scaling regime [33], as opposed to the (roughly) fixed value (partial shadowing) in the fixed-coupling case, and would lead to total gluon shadowing at very high rapidities if fluctuations were absent. The combination of the running of the coupling plus fluctuations would give total gluon shadowing at lower rapidities as compared to the fixed coupling case presented here. An extension of this work by the running coupling remains work for the future.

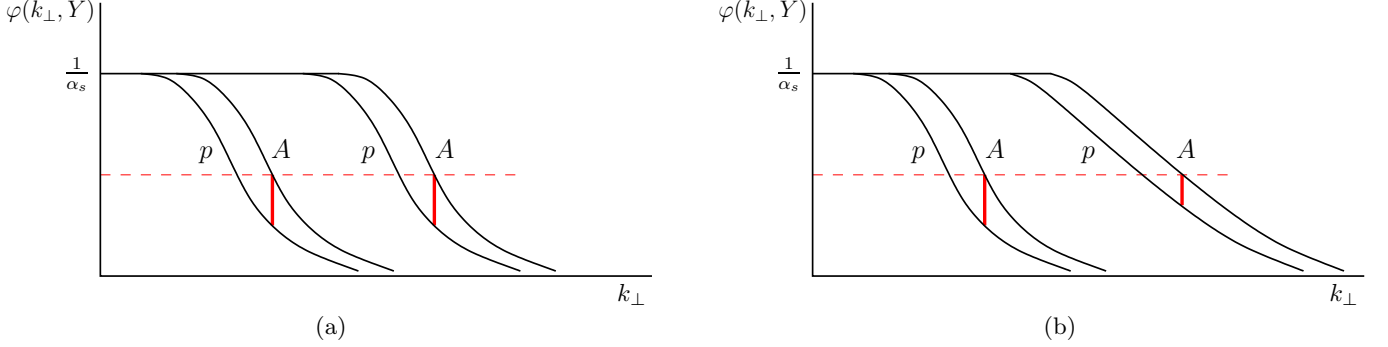


FIG. 2: The qualitative behaviour of the unintegrated gluon distribution of a nucleus (A) and a proton (p) at two different rapidities in the geometric scaling regime (a) and diffusive scaling regime (b).

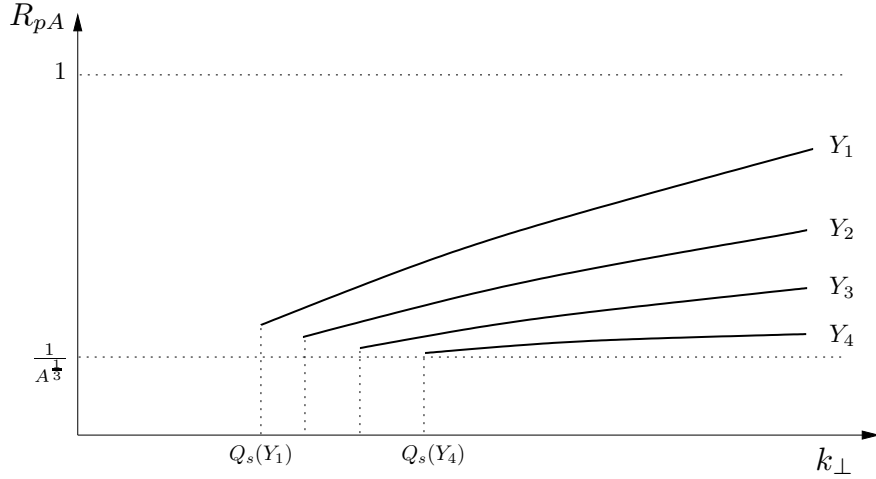


FIG. 3: The qualitative behaviour of the ratio  $R_{pA}$  as a function of  $k_{\perp}$  at four different rapidities,  $Y_1 \leq Y_2 \leq Y_3 \leq Y_4$ , in the diffusive scaling regime.  $R_{pA}$  is always smaller than one for values of  $k_{\perp}$  in the diffusive scaling regime.

### Acknowledgments

We would like to thank Al Mueller for valuable discussions. B. X. wishes to thank the Physics Department of the University of Bielefeld for hospitality during his visit when this work was being initialized. A. Sh. and M. K. acknowledge financial support by the Deutsche Forschungsgemeinschaft under contract Sh 92/2-1.

### APPENDIX A: MCLERRAN-VENUGOPALAN INITIAL CONDITION FOR THE PROTON

Also the proton can be described within the McLerran-Venugopalan model, as done for the nucleus in Sect. II B. The only change as compared to the description of the nucleus is a different saturation momentum for the proton due to the different initial conditions. It is reasonable to assume the following relation between their saturation momenta

$$\langle Q_s(A, Y) \rangle^2 = A^{1/3} \langle Q_s(p, Y) \rangle^2 \quad (\text{A1})$$

or in terms of  $\langle \rho_s(A, Y) \rangle = \ln(\langle Q_s(A, Y) \rangle^2 / k_0^2)$ ,

$$\langle \rho_s(A, Y) \rangle = \langle \rho_s(p, Y) \rangle + \ln A^{1/3}. \quad (\text{A2})$$

This relation holds formally if one extrapolates the McLerran-Venugopalan model, which was constructed for a large nucleus, down to  $A = 1$ . So, to get the expressions for the proton from the ones given for the nucleus in the previous sections, one has to replace  $\langle Q_s(A, Y) \rangle^2$  by  $\langle Q_s(p, Y) \rangle^2$ , or, the difference  $\Delta \rho_s$  in Eq. (37) by

$$\Delta \rho_s^{MV} \equiv \langle \rho_s(A, Y) \rangle - \langle \rho_s(p, Y) \rangle = \ln A^{1/3}. \quad (\text{A3})$$

With this difference, the ratio in the geometric scaling region, as compared to (45), now reads

$$R_{pA}^{h,\varphi}(k_\perp, Y, A) = \frac{1}{A^{\frac{1}{3}(1-\gamma_c)}} \frac{\ln \left( \frac{k_\perp^2}{\langle Q_s(A, Y) \rangle^2} \right) + \frac{1}{\gamma_c}}{\ln \left( \frac{k_\perp^2}{\langle Q_s(A, Y) \rangle^2} \right) + \ln A^{\frac{1}{3}} + \frac{1}{\gamma_c}} \quad (\text{A4})$$

and shows the same features (partial gluon shadowing and  $k_\perp^2$  and  $Y$  independence for  $\ln k_\perp^2 / \langle Q_s(A, Y) \rangle \gg \ln A^{1/3}$ ) as the result in Eq. (45). In the diffusive scaling regime, instead of Eq.(46), now one obtains

$$R_{pA}^h = \frac{1}{A^{\frac{1}{3}(1-\frac{\ln A^{1/3}}{2\sigma^2})}} \left[ \frac{k_\perp^2}{\langle Q_s(A, Y) \rangle^2} \right]^{\frac{\ln A^{1/3}}{\sigma^2}}, \quad (\text{A5})$$

and instead of Eq. (47)

$$R_{pA}^\varphi = \frac{1}{A^{\frac{1}{3}(1-\frac{\ln A^{1/3}}{2\sigma^2})}} \left[ \frac{k_\perp^2}{\langle Q_s(A, Y) \rangle^2} \right]^{\frac{\ln A^{1/3}}{\sigma^2}} \frac{\left[ \ln \left( \frac{k_\perp^2}{\langle Q_s(A, Y) \rangle^2} \right) + \ln A^{\frac{1}{3}} \right]^2}{\left[ \ln \left( \frac{k_\perp^2}{\langle Q_s(A, Y) \rangle^2} \right) \right]^2}, \quad (\text{A6})$$

which show the same universal features for the ratio  $R_{pA}^{h,\varphi}$ , total shadowing at  $Y \rightarrow \infty$  and a decreasing  $k_\perp^2$  dependence with rising  $Y$ , as discussed in the previous section.

## APPENDIX B: GLUON DISTRIBUTION IN THE SATURATION REGION

We calculate the gluon distribution in the saturation region, where  $k_\perp^2 < Q_s^2$ , by solving the Kovchegov equation [9] at high rapidities. The Kovchegov equation in momentum space, at a fixed impact parameter, reads [9]

$$\frac{\partial \phi(\rho, Y)}{\bar{\alpha}_s \partial Y} = \chi(-\partial_\rho) \phi(\rho, Y) - \phi^2(\rho, Y), \quad (\text{B1})$$

where  $\rho = \ln \frac{k_\perp^2}{k_0^2}$  and  $\phi(\rho, Y) = \frac{(2\pi)^2 \alpha_s}{N_c} \varphi_A(k_\perp, Y)$  the Weizsacker-Williams gluon distribution defined in Eq. (5) (apart from the prefactor). It is convenient to look for a solution to the Kovchegov equation in the saturation regime in the form

$$\phi(\rho, Y) = \int_{c-i\infty}^{c+i\infty} \frac{d\gamma}{2\pi i} \phi(\gamma) \exp[-\gamma(\rho - v\bar{\alpha}_s Y)], \quad (\text{B2})$$

$$= \int_{c-i\infty}^{c+i\infty} \frac{d\gamma}{2\pi i} \phi(\gamma) \exp \left[ -\gamma \ln \left( \frac{k_\perp^2}{Q_s^2(Y)} \right) \right] \quad (\text{B3})$$

with  $Q_s^2(Y) = k_0^2 \exp[\bar{\alpha}_s v Y]$ . In the saturation regime,  $\ln \left( \frac{k_\perp^2}{Q_s^2(Y)} \right) < 0$ , the contour integral has to be closed to the left and form a counterclockwise path in order to enclose all the poles of  $\phi(\gamma)$ . The first and most important pole of  $\phi(\gamma)$  is at  $\gamma = 0$ . Using the Laurent expansion of  $\phi(\gamma)$  at  $\gamma = 0$ , which is  $\phi(\gamma) = \sum_{n=-\infty}^{\infty} a_n \gamma^n$ , in Eq.(B1), one can immediately spot that there must be a cutoff of  $n$  at  $n = -2$ . Thus,  $\phi(\gamma)$  can be written as

$$\phi(\gamma) = \frac{a_1}{\gamma^2} + \frac{a_2}{\gamma} + a_3 + f(\gamma) \quad (\text{B4})$$

with  $f(0) = 0$ . The function  $f(\gamma)$  would have some poles at  $\gamma = -\gamma_i$  where  $\gamma_i > 0$ , which however do generate small contributions like  $\left(\frac{k_\perp^2}{Q_s^2(Y)}\right)^{\gamma_i}$  to  $\phi(\rho, Y)$  in the saturation region. Therefore the most important contributions are from  $\phi_0(\gamma) \equiv \phi(\gamma) - f(\gamma)$ .

It is now straightforward to see that

$$\phi_0(\rho, Y) = a_1 \ln \frac{Q_s^2(Y)}{k_\perp^2} + a_2, \quad (\text{B5})$$

$$\frac{\partial \phi_0(\rho, Y)}{\alpha_s \partial Y} = a_1 v, \quad (\text{B6})$$

$$\chi(-\partial_\rho) \phi_0(\rho, Y) = \frac{1}{2} a_1 \left( \ln \frac{Q_s^2(Y)}{k_\perp^2} \right)^2 + a_2 \ln \frac{Q_s^2(Y)}{k_\perp^2} + a_3 + \sum_{n=1}^{\infty} \left( \frac{a_1}{n^2} - \frac{a_2}{n} + a_3 \right) \left( \frac{k_\perp^2}{Q_s^2(Y)} \right)^n \quad (\text{B7})$$

where the last term in (B7) comes from the residues of  $\chi(\gamma)$  at  $\gamma = -n$  with  $n = 1, 2, \dots$ . Up to some small correction of order  $\frac{k_\perp^2}{Q_s^2(Y)}$ , Eq.(B1) is solved by  $\phi_0(\rho, Y) = a_1 \ln \frac{Q_s^2(Y)}{k_\perp^2} + a_2$  with  $a_1 = \frac{1}{2}$  and  $\frac{1}{2}v = a_3 - a_2^2$ . Moreover one can set  $a_2 = 0$  and get  $a_3 = \frac{1}{2}v$ . Finally, one obtains the approximate solution to the Kovchegov equation,  $\phi(\rho, Y) = \frac{1}{2} \ln \frac{Q_s^2(Y)}{k_\perp^2} + \mathcal{O}\left(\frac{k_\perp^2}{Q_s^2(Y)}\right)$ , and the gluon distribution as defined in Eq. (5) takes the form in the saturation regime as cited in Eq.(39)

$$\varphi_A(k_\perp, Y) = \frac{N_c}{2(2\pi)^2 \alpha_s} \left[ \ln \frac{Q_s^2(Y)}{k_\perp^2} + \mathcal{O}\left(\frac{k_\perp^2}{Q_s^2(Y)}\right) \right]. \quad (\text{B8})$$

The gluon distribution as defined in Eq.(2) reads in the saturation regime

$$h_A(k_\perp, Y) \propto \frac{N_c}{2(2\pi)^2 \alpha_s} \frac{k_\perp^2}{Q_s^2(Y)}, \quad (\text{B9})$$

and is obtained from Eq. (B8), the higher order correction term, by using the relation in Eq. (6).

- 
- [1] A. H. Mueller, A. I. Shoshi and S. M. H. Wong, Nucl. Phys. B **715** 440 (2005).
  - [2] E. Iancu and D. N. Triantafyllopoulos, Nucl. Phys. A **756** (2005) 419.
  - [3] E. Iancu and D. N. Triantafyllopoulos, Phys. Lett. B **610** 253 (2005).
  - [4] S. Munier and R. Peschanski, Phys. Rev. Lett. **91** (2003) 232001; Phys. Rev. D **69** (2004) 034008.
  - [5] E. Iancu, A. H. Mueller and S. Munier, Phys. Lett. B **606** (2005) 342.
  - [6] A. H. Mueller and A. I. Shoshi, Nucl. Phys. B **692** (2004) 175.
  - [7] J. Jalilian-Marian, A. Kovner, A. Leonidov and H. Weigert, Nucl. Phys. B **504** 415 (1997); Phys. Rev. D **59** 014014 (1999); J. Jalilian-Marian, A. Kovner and H. Weigert, Phys. Rev. D **59**, 014015 (1999); E. Iancu, A. Leonidov and L. D. McLerran, Phys. Lett. B **510** 133 (2001); Nucl. Phys. A **692** 583 (2001); H. Weigert, Nucl. Phys. A **703** 823 (2002).
  - [8] I. Balitsky, Nucl. Phys. B **463** 99 (1996); Phys. Rev. Lett. **81** 2024 (1998); Phys. Lett. B **518** 235 (2001).
  - [9] Y. V. Kovchegov, Phys. Rev. D **60** 034008 (1999); Phys. Rev. D **61** 074018 (2000).
  - [10] Y. Hatta, E. Iancu, C. Marquet, G. Soyez and D. N. Triantafyllopoulos, Nucl. Phys. A **773**, 95 (2006).
  - [11] A. Kovner and M. Lublinsky, Phys. Rev. D **71** 085004 (2005).
  - [12] E. Levin and M. Lublinsky, Nucl. Phys. A **763** (2005) 172.
  - [13] R. Enberg, K. Golec-Biernat and S. Munier, Phys. Rev. D **72**, 074021 (2005).
  - [14] E. Brunet, B. Derrida, A. H. Mueller and S. Munier, "A phenomenological theory giving the full statistics of the position of fluctuating pulled fronts," Phys. Rev. E **73** (2006) 056126.
  - [15] S. Munier, "Dense-dilute factorization for a class of stochastic processes and for high energy QCD," arXiv:hep-ph/0608036.
  - [16] A. I. Shoshi and B. W. Xiao, Phys. Rev. D **73** (2006) 094014.
  - [17] S. Bondarenko, L. Motyka, A. H. Mueller, A. I. Shoshi and B. W. Xiao, "On the equivalence of Reggeon field theory in zero transverse dimensions and reaction-diffusion processes," arXiv:hep-ph/0609213.
  - [18] J. P. M. Blaizot, E. Iancu and D. N. Triantafyllopoulos, "A zero-dimensional model for high-energy scattering in QCD," arXiv:hep-ph/0606253.
  - [19] E. Iancu, J. T. de Santana Amaral, G. Soyez and D. N. Triantafyllopoulos, "One-dimensional model for QCD at high energy," arXiv:hep-ph/0611105.
  - [20] C. Marquet, R. Peschanski and G. Soyez, Phys. Rev. D **73** (2006) 114005.
  - [21] G. Soyez, Phys. Rev. D **72** (2005) 016007.

- [22] M. Kozlov and E. Levin, Nucl. Phys. A **779** (2006) 142.
- [23] S. Bondarenko and L. Motyka, arXiv:hep-ph/0605185.
- [24] A. Kovner, M. Lublinsky and H. Weigert, “Treading on the cut: Semi inclusive observables at high energy,” arXiv:hep-ph/0608258.
- [25] A. I. Shoshi and B. W. Xiao, “Diffractive dissociation including pomeron loops in zero transverse dimensions,” arXiv:hep-ph/0605282.
- [26] M. Kozlov, E. Levin, V. Khachatryan and J. Miller, “The BFKL pomeron calculus in zero transverse dimensions: Diffractive processes and survival probability for central diffractive production,” arXiv:hep-ph/0610084.
- [27] E. Iancu, C. Marquet and G. Soyez, Nucl. Phys. A **780** (2006) 52.
- [28] A. Kovner and M. Lublinsky, “One gluon, two gluon: Multigluon production via high energy evolution,” arXiv:hep-ph/0609227.
- [29] R. Baier, A. Kovner and U. A. Wiedemann, Phys. Rev. D **68**, 054009 (2003).
- [30] D. Kharzeev, Y. V. Kovchegov and K. Tuchin, Phys. Rev. D **68**, 094013 (2003).
- [31] J. Jalilian-Marian, Y. Nara and R. Venugopalan, Phys. Lett. B **577**, 54 (2003).
- [32] J. P. Blaizot, F. Gelis and R. Venugopalan, Nucl. Phys. A **743**, 13 (2004).
- [33] E. Iancu, K. Itakura and D. N. Triantafyllopoulos, Nucl. Phys. A **742**, 182 (2004).
- [34] J. L. Albacete, N. Armesto, A. Kovner, C. A. Salgado and U. A. Wiedemann, Phys. Rev. Lett. **92**, 082001 (2004).
- [35] R. Baier, A. H. Mueller and D. Schiff, Nucl. Phys. A **741**, 358 (2004).
- [36] A. H. Mueller, Nucl. Phys. A **724** (2003) 223.
- [37] D. Kharzeev, E. Levin and L. McLerran, Phys. Lett. B **561** (2003) 93.
- [38] M. Braun, Eur. Phys. J. C **16**, 337 (2000).
- [39] Y. V. Kovchegov, Phys. Rev. D **54** (1996) 5463; Phys. Rev. D **55** (1997) 5445.
- [40] Y. V. Kovchegov and A. H. Mueller, Nucl. Phys. B **529** (1998) 451.
- [41] J. Jalilian-Marian, A. Kovner, L. D. McLerran and H. Weigert, Phys. Rev. D **55** (1997) 5414.
- [42] E. Iancu, K. Itakura and L. McLerran, Nucl. Phys. A **708** (2002) 327.
- [43] A. H. Mueller and D. N. Triantafyllopoulos, Nucl. Phys. B **640**, 331 (2002).
- [44] L. D. McLerran and R. Venugopalan, Phys. Rev. D **49** (1994) 3352; Phys. Rev. D **49** (1994) 2233; Phys. Rev. D **50** (1994) 2225.
- [45] C. Marquet, G. Soyez and B. W. Xiao, Phys. Lett. B **639**, 635 (2006).
- [46] A. M. Stasto, K. Golec-Biernat and J. Kwiecinski, Phys. Rev. Lett. **86** (2001) 596.